Erschienen in: Applied Physics Letters ; 110 (2017), 3. - 031904
https://dx.doi.org/10.1063/1.4974491

Acoustic beam splitting at low GHz frequencies in a defect-free phononic crystal

Yuning Guo,[1,a)] Delia Brick,[1] Martin Großmann,[1] Mike Hettich,[1] and Thomas Dekorsy[1,2]
[1]*Department of Physics, University of Konstanz, 78457 Konstanz, Germany*
[2]*Institute of Technical Physics, German Aerospace Center, Pfaffenwaldring 38 40, 70568 Stuttgart, Germany*

The directional waveguiding in a 2D phononic crystal is simulated based on the analysis of equifrequency contours. This approach is utilized to investigate acoustic beam splitting in a defect-free nanostructure in the low GHz range. We find relaxed limitations regarding the source parameters compared to similar approaches in the sonic regime. Finally, we discuss the possibility to design an acoustic interferometer device at the nanoscale at GHz frequencies. *Published by AIP Publishing.*

Besides the interest in the bandgap and defect-based waveguiding of phononic crystals (PnCs), waveguiding based on the shape of equifrequency contours (EFCs) has recently attracted attention.[1–3] The development of PnCs and exploiting directional waveguiding therein have enabled a wide range of possible applications.[4–7] However, many concepts and basic applications have so far been demonstrated in the sonic regime while the realization of hypersonic applications in the GHz regime still remains challenging.[5,8] Here, we apply some of the established concepts for the design of directional waveguiding in order to study possible designs for devices in the low GHz range.

Self-collimation enables guided wave propagation in PnCs without a structurally defined waveguide, which is convenient for on-chip acoustic integrated circuits.[9,10] Taking advantage of self-collimation, devices such as imaging lenses, acoustic diodes, acoustic logic gates, and wavelength division multiplexers can be realized.[11–15] Since collimated waves only propagate in one direction, which limits the application in integrated acoustic devices, the splitting and bending of them are significant problems to be solved. Several approaches have been presented that show acoustic beam splitting capabilities utilizing either defect-based[10,13,16–18] or defect-free concepts.[19,20] A defect-free structure is highly desirable due to advantages in actual fabrication at the nanoscale when hypersonic crystals are concerned, which can strongly reduce tedious technological processes and potentially improve the precision of the devices. Many of the already explored crystals and concepts for defect-free beam splitting devices show certain limitations, especially regarding the spatial size of the excitation source.[20] Regarding laser or transducer induced acoustic wave excitation for hypersound, this poses a severe limitation and needs to be addressed.

In the following, we will discuss a defect-free acoustic beam splitting device of μm size in the low GHz frequency regime, which has relaxed limitations regarding the excitation source. Our design approach shows that the experimental realization of GHz acoustic beam splitting devices is still challenging but is within reach. We will discuss the influence of the source parameters and a possible application of the highly directional beam splitting as an acoustic interferometer at the nanoscale.

The PnC consists of a square array of cylindrical silicon pillars in air. The Young's modulus E, Poisson ratio σ, and density ρ of silicon are set as 165 GPa, 0.27, and 2330 kg/m^3, respectively.[21] The simulation is calculated in a frequency range from 0 to 3 GHz based on the finite element method (FEM) using Comsol. The lattice constant a is 200 nm and the radius of the pillars r is 60 nm. The calculation region is comprised of 36 × 37 inclusions, and perfectly matched layers (PMLs) are set in front and the rear of the PnC in order to suppress artificial back reflections. An acoustic Gaussian source with an full width at half maximum (FWHM) of 100 nm along the y-direction, which is placed 200 nm in front of the PnC, is used as the excitation source.

Figure 1(a) shows the band structure of the PnC in the first Brillouin zone. The red and blue lines mark the frequencies we will focus on. Figure 1(b) shows the pressure field of the PnC at 1.60 GHz, which undergoes self-collimation and zero-angle refraction.[9,10] The inset corresponds to EFCs of the 3rd band from 1.28 GHz to 1.72 GHz, and the red contour with zero curvature along the ΓX direction represents a frequency of 1.60 GHz. The collimated waves propagate non-diffractive because their Bloch wave vectors lying on the flat segment of the dispersion curve have equal longitudinal components and thus do not dephase during propagation.[3] Beam splitting upon leaving the PnC is also observed, which is attributed to multiple Bloch modes satisfying phase-matching conditions and leads to higher order refracted modes.[22–25] Figure 1(c) depicts the extended Brillouin zone of the EFCs of the 1st band from 0.40 GHz to 0.76 GHz and the blue contours at 0.66 GHz, which exhibit flat curvatures along the ΓM direction. The propagation direction of acoustic waves within the PnC is governed by the gradient at each point of the EFC, and thus the refraction is influenced by the shape of the EFCs and their positions.[22] When the incident wave propagates along the ΓX direction at 0.66 GHz, the wave vector of the refracted wave inside the PnC is first refracted at an angle of 45 degree, which is along the ΓM direction and then propagates as a self-collimated wave. The corresponding pressure field shown in Fig. 1(d) confirms the

[a)]Author to whom correspondence should be addressed. Electronic mail: yuning.guo@uni konstanz.de

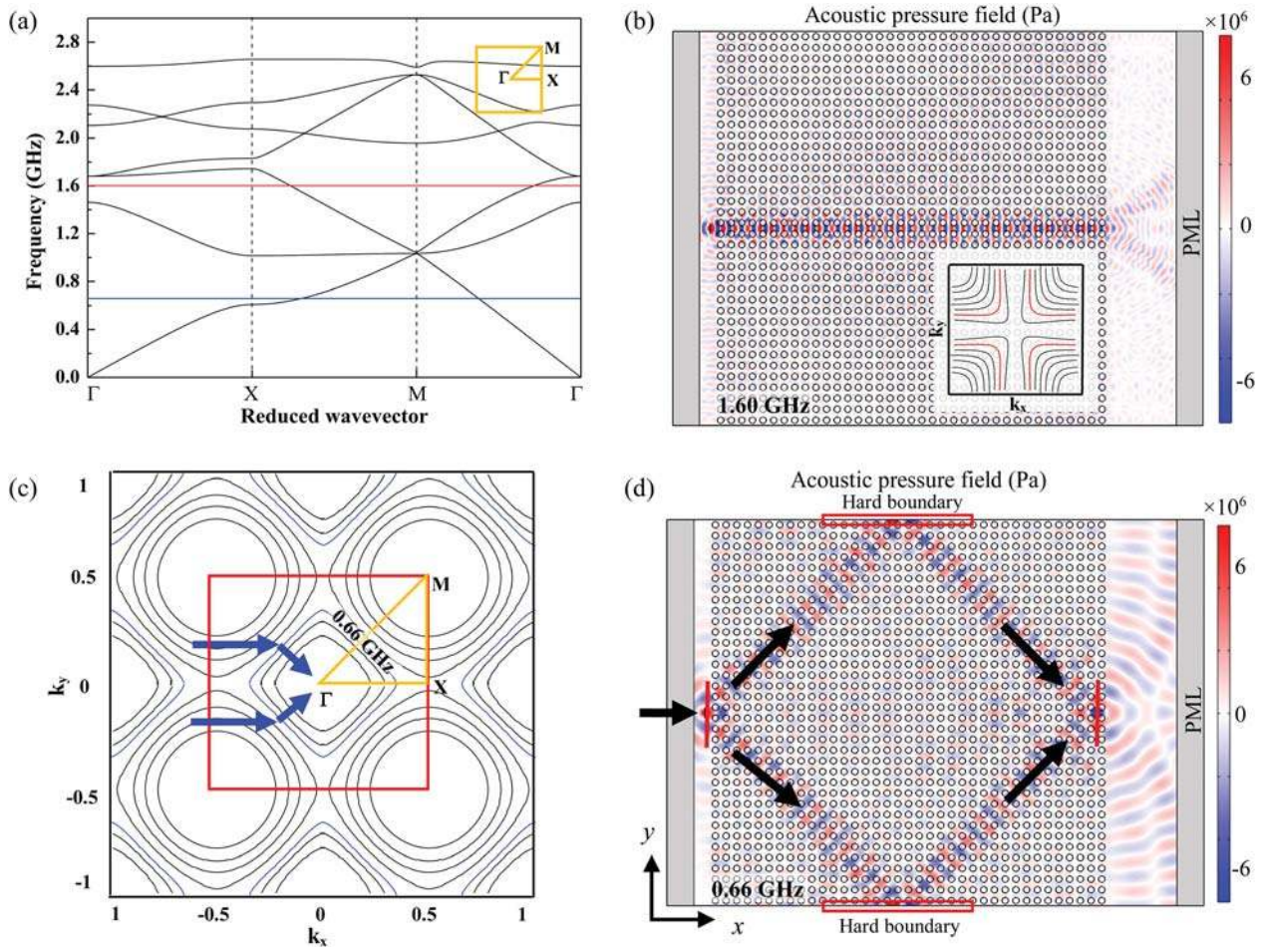

FIG. 1. (a) Band structure of a PnC of silicon inclusions in air, the coloured lines mark the frequencies we are interested in; (b) pressure field of the PnC at 1.60 GHz, the inset corresponds to the EFCs of the 3rd band and the red contours represent 1.60 GHz; (c) the extended Brillouin zone of the EFCs of the 1st band (in unit of $2\pi/a$) and the blue contours represent 0.66 GHz; (d) pressure field of the PnC at 0.66 GHz, the arrows represent the propagation directions of acoustic waves; the red lines indicate the input and output.

analysis of the EFCs at 0.66 GHz. When the acoustic wave impinges upon the PnC, the acoustic beams are split into two separate beams, which exhibit equal intensities and form an angle of $\pm 45°$ with the propagation axis. The hard boundaries here act as mirrors for the self-collimated beams propagating along the ΓM direction. Since the two reflected beams are in phase, constructive interference is obtained at the intersection area near the output. This design already resembles an acoustic interferometer. We want to emphasize here that a rotation of the PnC by 45° interchanges the propagation behavior of the 0.66 and 1.60 GHz modes due to the exchange in the ΓX and ΓM directions.

It is important to note here that all the Bloch modes can couple to and propagate within the PnC as no directional bandgap exists in the ΓM direction. Therefore, there is no limitation of the source size in order to achieve beam splitting, contrary to previously proposed designs in the sonic range.[20] In other words, the acoustic beam splitting can be obtained within a wide range of possible sizes of the excitation source, while the details of the beam splitting are influenced by the parameters of the excitation source, which we will discuss in more detail later on.

The distributions of the pressure of the input and output of the PnC at 0.66 GHz, i.e., the beam splitting case, are analyzed with respect to their intensity and width of the central fringe in Fig. 2. The pressure distributions are taken from the red lines marked in Fig. 1(d). The pressure distributions calculated in the frequency domain take into account losses due to waves leaving the PnC as well as cumulative effects due to waves remaining in the crystal because of multiple reflections and scattering. The FWHM of 280 nm at 0.66 GHz for the central fringes from the input and output regions shows only small deviations, in this case. Self-collimation

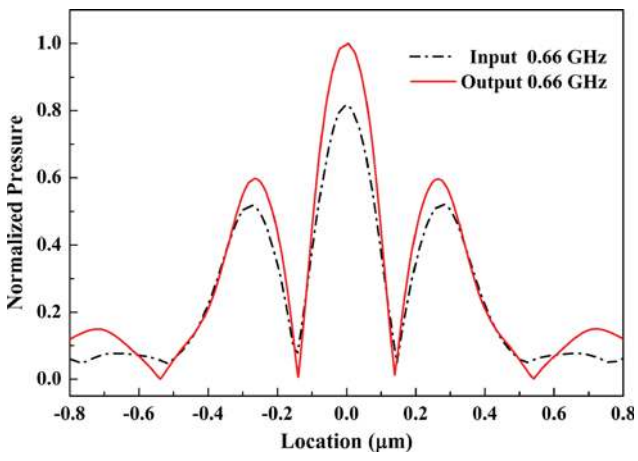

FIG. 2. The normalized pressure at the input and output versus the location.

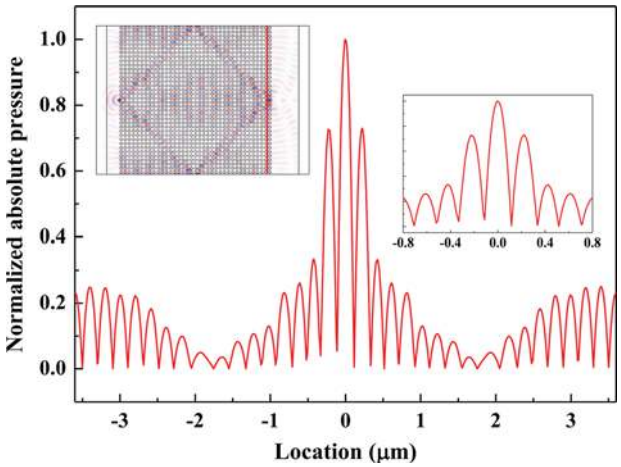

FIG. 3. The normalized pressure at the output at 0.66 GHz with a source PnC distance of 0.1a. The left inset shows the corresponding pressure field while the right one shows the center region.

suppresses the broadening of propagating acoustic waves within the PnC. Although the propagating beams are scattered within the PnC, the intensity of the output is larger than the input at 0.66 GHz due to the constructive interference of the two reflected waves. The half-width of the central fringe at 0.66 GHz is 0.41λ, which is less than the half-wavelength of propagating waves in the PnC; we like to note that this finding is of possible interest for applications in acoustic super-resolution imaging, e.g., flexible superlenses at high frequency as well as sensing and detecting objects at the sub-wavelength level.[26–28]

The key point here is that the beam splitting is achieved for a wide range of parameters of the excitation source. However, the interference phenomena in the overlap region depend on the details of the source position and size. Figure 3 shows the pressure distribution of the output at 0.66 GHz where the source is placed closer to the PnC (source-PnC distance is 0.1a); the left inset shows the corresponding pressure field and the right one shows the center region in more detail. The strong signal in the center region at the output and the clearly acoustic wave within the area surrounded by split beams can be observed from the pressure field. When the distance between the source and the PnC is less than the lattice constant, the amplitude distribution of the pressure in the overlap region resembles double-slit Fraunhofer diffraction, which is given by single slit diffraction and double slit interference. Thus, we believe that the pressure distribution here shows the combination of the diffraction of the whole source and the interference of the two split beams. This design is similar to a Mach-Zehnder interferometer, which produces two-wave interference by splitting the amplitude of the wave. The respective contributions of diffraction and interference affect the pressure distribution of the output. Thus, we will discuss the possibilities to tune them independently of each other, which allows influencing the pressure distribution in the overlap region, which is also beneficial to optimize the acoustic interferometer.

When the excitation source is in close proximity to the PnC, strong diffraction occurs, which resembles optical counterpart, and thus disturbs the observation of interference signals. An increase in the source-PnC distance causes a broadening of the splitting beams due to the diffusive behaviour of the excited waves, which in turn results in a larger overlap area. The published work shows that the super-resolution can be obtained when the source is closer to the PnC due to the fact that more evanescent waves couple to a bound mode of the crystal.[27,28] In our case, the width of the center fringes is 231 nm with half-width 0.27λ, which is narrower than the normal source-PnC distance condition and agrees with the conclusions in Ref. 28, and hence provides the possibility of super-resolution imaging. However, the amplitude of the center fringe decreases and secondary fringes increase, which poses a disadvantage for super-resolution imaging.

The beam splitting capabilities of the PnC are investigated by exciting the PnC with line sources at different locations and with different sizes. As shown in Fig. 4(a), when the size of the excitation source is just several times that of

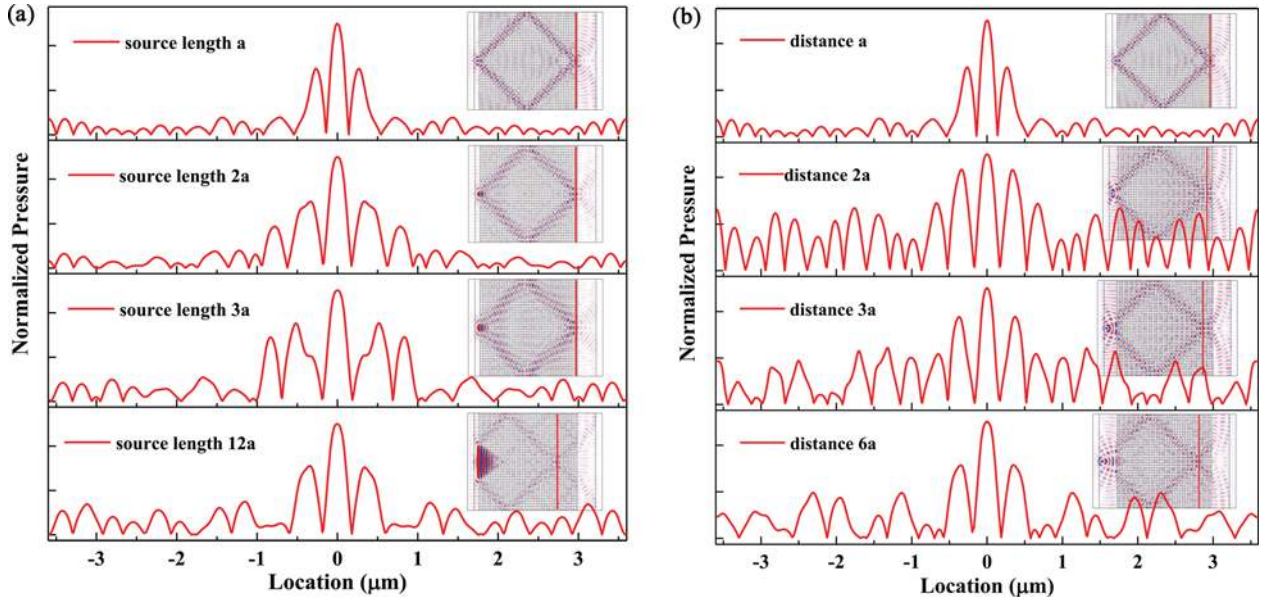

FIG. 4. The normalized pressure at the collimated beams overlap position and the corresponding pressure fields at 0.66 GHz with (a) different source sizes; and (b) different source PnC distances.

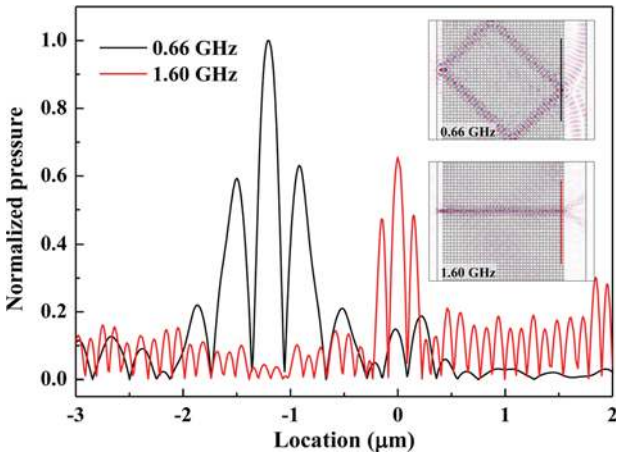

FIG. 5. The normalized pressure at the output with the shifted excitation source.

the lattice constant, with increasing the size, the propagating beams within the PnC broaden, and therefore, the overlap region increases and the disturbance of the pressure from side lobes on the center fringe at the output position increases. When the size of the source is comparable to the lattice constant, its length in reciprocal space is similar too, which guarantees that the excited acoustic wave can couple well to the PnC and reduces the disadvantageous influence of round corners in the EFC. When the size of the source is more than five times larger than the lattice constant, the beam splitting still can be clearly observed, while the location of the overlapping region shifts and the amplitude of the splitting beams decreases as only outer parts of the acoustic waves reached in the PnC contribute to the split beams. The strong pressure distribution near the source, which is similar to a plane wave, is caused by the superposition of diffractive waves induced by the long excitation source. With increasing the source-PnC distance (source length is a), the intersection point shifts closer to the excitation source and the beam splitting quality deteriorates as shown in Fig. 4(b). Although the diffraction is not as strong as in Fig. 3, the beams that reach the PnC are not perfectly collimated anymore, which lead to the increase in noises to the central fringes and decrease in the intensities of split beams. Therefore, the location and size of the excitation source are two critical factors in the beam splitting quality of the PnC at a given frequency.

So far, the self-collimated and split beams intersect at the same output position of the crystal. This might pose problems or might be unwanted in actual devices. One possibility to achieve a frequency dependent spatial separation can be realized by adjusting the source position. When the excitation source shifts along the y axis, the distance $3a$ from the center along the y direction, as shown in Fig. 5, the intersection point of the reflected waves shifts down the same distance $3a$ while the output of the self-collimated beam stays at the original position along the y-direction of the excitation source. Therefore, the distance between the two outputs is $6a$, which provides a convenient way to separate the output signals.

In principle, EFCs with different shapes can be used to change the angle between the split beams. Since the self-collimation is obtained from EFCs determined by the band structure, the beam splitting can be achieved in both hole-type and pillar-type PnCs. This effect still persists when the size of the PnC system scales to μm or mm and therefore extends the possible design applications to a wide frequency range.

In conclusion, by tailoring the EFCs in a 2D PnC, directional waveguiding is obtained and a defect-free beam splitting device in the low GHz frequency is demonstrated. The relaxed limitations of the excitation source provide a possible way to realize a beam splitting device in the GHz frequency range. With appropriate settings of the location and the size of the source, the diffraction of acoustic waves can be tuned, which in turn influences the pressure distribution in the overlap region and thus the interference of the overlapping beams. Our approach can be used to design devices based on acoustic beam splitting like acoustic sensors, acoustic integrated circuits, and nano-electromechanical systems.

This work was supported by the German Research Foundation (DFG) through the SFB 767. Y. Guo gratefully acknowledges the financial support from the China Scholarship Council (CSC).

[1]A. Sukhovich, L. Jing, and J. H. Page, Phys. Rev. B **77**, 014301 (2008).
[2]J. Zhao, R. Marchal, B. Bonello, and O. Boyko, Appl. Phys. Lett. **101**, 261905 (2012).
[3]E. M. Hamham, N. Jiménez, R. Picó, V. J. Sánchez Morcillo, L. M. García Raffi, and K. Staliunas, Phys. Rev. B **92**, 054302 (2015).
[4]M. Maldovan, Nature **503**, 209 (2013).
[5]R. Olsson III and I. El Kady, Meas. Sci. Technol. **20**, 012002 (2009).
[6]A. H. Safavi Naeini, J. T. Hill, S. Meenehan, J. Chan, S. Groblacher, and O. Painter, Phys. Rev. Lett. **112**, 153603 (2014).
[7]M. I. Hussein, M. J. Leamy, and M. Ruzzene, Appl. Mech. Rev. **66**, 040802 (2014).
[8]T. W. Liu, Y. C. Tsai, Y. C. Lin, T. Ono, S. Tanaka, and T. T. Wu, AIP Adv. **4**, 124201 (2014).
[9]I. Pérez Arjona, V. J. Sánchez Morcillo, J. Redondo, V. Espinosa, and K. Staliunas, Phys. Rev. B **75**, 014304 (2007).
[10]D. W. Prather, S. Shi, J. Murakowski, G. J. Schneider, A. Sharkawy, C. Chen, B. Miao, and R. Martin, J. Phys. D: Appl. Phys. **40**, 2635 (2007).
[11]C. Y. Chiang and P. G. Luan, J. Phys.: Condens. Matter **22**, 055405 (2010).
[12]X. F. Li, X. Ni, L. Feng, M. H. Lu, C. He, and Y. F. Chen, Phys. Rev. Lett. **106**, 084301 (2011).
[13]T. Zhang, Y. Cheng, J. Z. Guo, J. Y. Xu, and X. J. Liu, Appl. Phys. Lett. **106**, 113503 (2015).
[14]M. H. Lu, C. Zhang, L. Feng, J. Zhao, Y. F. Chen, Y. W. Mao, J. Zi, Y. Y. Zhu, S. N. Zhu, and N. B. Ming, Nat. Mater. **6**, 744 (2007).
[15]Q. B. Li, Z. Li, and R. X. Wu, Appl. Phys. Lett. **107**, 241907 (2015).
[16]A. Cicek, O. A. Kaya, and B. Ulug, Appl. Phys. Lett. **100**, 111905 (2012).
[17]O. A. Kaya, A. Cicek, A. Salman, and B. Ulug, Sensors Actuators, B **203**, 197 (2014).
[18]S. G. Lee, S. S. Oh, J. E. Kim, H. Y. Park, and C. S. Kee, Appl. Phys. Lett. **87**, 181106 (2005).
[19]J. Wen, D. Yu, L. Cai, and X. Wen, J. Phys. D: Appl. Phys. **42**, 115417 (2009).
[20]A. Cicek, O. A. Kaya, and B. Ulug, Chin. Phys. B **22**, 114301 (2013).
[21]See https://www.memsnet.org/material/siliconsibulk/ for material properties.
[22]J. Bucay, E. Roussel, J. Vasseur, P. Deymier, A. Hladky Hennion, Y. Pennec, K. Muralidharan, B. Djafari Rouhani, and B. Dubus, Phys. Rev. B **79**, 214305 (2009).
[23]J. Vasseur, B. Morvan, A. Tinel, N. Swinteck, A. C. Hladky Hennion, and P. A. Deymier, Phys. Rev. B **86**, 134305 (2012).
[24]N. Swinteck, S. Bringuier, J. F. Robillard, J. Vasseur, A. Hladky Hennion, K. Runge, and P. Deymier, J. Appl. Phys. **110**, 074507 (2011).
[25]N. Swinteck, J. F. Robillard, S. Bringuier, J. Bucay, K. Muralidharan, J. Vasseur, K. Runge, and P. Deymier, Appl. Phys. Lett. **98**, 103508 (2011).
[26]C. Luo, S. G. Johnson, J. Joannopoulos, and J. Pendry, Phys. Rev. B **68**, 045115 (2003).
[27]J. H. Page, Z. Liu, and S. Yang, in PHONONICS 2015 Brillouin Paper, Phononics 2015, Paris, France (2015).
[28]A. Sukhovich, B. Merheb, K. Muralidharan, J. Vasseur, Y. Pennec, P. Deymier, and J. Page, Phys. Rev. Lett. **102**, 154301 (2009).